ARTICLE

Phase Distribution of Al$_2$O$_3$ Thin Films on Rare Earth-Modified Fe-Al Layer Surface

Yin Qi,   Yuan Xiaoming,   Zhang Jiantong,   Feng Fan,   Yang Hongguang

China Institute of Atomic Energy, Beijing 102413, China

Abstract: Fe-Al/Al$_2$O$_3$ composite coating was prepared through rare earth-modified aluminizing and in-situ oxidation at 760 °C. The microstructure and phase distribution of the aluminizing layer and oxide film were investigated. Results show that the rare earth-modified aluminizing layer can be divided into three layers: an outer aluminizing layer, a transition layer, and an inner diffusion layer. The aluminizing layer is predominantly composed of FeAl phase and Fe$_3$Al phase. Notably, the FeAl phase is primarily concentrated in the outer layer of aluminizing layer, providing favorable conditions for selective oxidation of the Al$_2$O$_3$ oxide film. The surface of oxide film exhibits the α-Al$_2$O$_3$ ridge structure. Additionally, the presence of Ce oxide on the surface is attributed to the outward diffusion of Ce and its preferential reaction with O$_2$ during the initial oxidation stage. The oxide film can be divided into two layers, namely a pure α-Al$_2$O$_3$ layer and a transition layer which is mainly composed of α-Fe(Al) and mixed oxides of Al, Fe, and Ce.

Key words: rare earth modification; aluminizing layer; oxide film; phase distribution

Controlled nuclear fusion is a promising long-term solution to satisfy the future energy demands. The deuterium-tritium fuel cycle can achieve sustainable supply of nuclear fusion energy. However, the permeability and radioactivity of tritium restrict its further application. Tritium can easily penetrate the structural materials, thereby causing nuclear pollution. Therefore, strict anti-tritium measures should be conducted. Currently, the most direct and effective approach for the tritium-related risk reduction is to apply tritium permeation barrier (TPB) on the surface of cladding structure. TPB serves as the protective shield, preventing the tritium penetration and potential environment pollution.

The selection of tritium-resistant coating materials has been conducted over the years. The mainstream tritium-resistant coatings can be categorized into oxide coatings (Al$_2$O$_3$, Y$_2$O$_3$, Cr$_2$O$_3$, Er$_2$O$_3$, SiO$_2$, ZrO$_2$)[1], titanium-based ceramic coatings (TiN, TiC, TiC/TiN)[2], silicide coatings (SiC, Si$_3$N$_4$, SiC/Si$_3$N$_4$)[3-4], and aluminizing layers (FeAl/Al$_2$O$_3$, AlN)[5]. Among them, Al$_2$O$_3$ coating attracts much attention due to its exceptional properties, such as high permeation reduction factor, high resistivity, excellent high-temperature resistance, and outstanding compatibility with lithium lead[6-7]. However, a significant challenge of Al$_2$O$_3$ coating lies in the substantial difference in linear thermal expansion coefficients between the metal substrate and Al$_2$O$_3$ layer. This disparity can cause thermal mismatch issues and eventually lead to the delamination or detachment of the coating. Therefore, a viable solution involving the formation of Fe-Al transition layer with gradient function between the substrate and Al$_2$O$_3$ coating has been proposed. This transition layer has designed composition and structure to alleviate the thermal mismatch between substrate and Al$_2$O$_3$ coating. Moreover, it promotes the reactions between oxygen atoms and other atoms, thereby facilitating the Al$_2$O$_3$ formation during service. In this case, the composite coating exerts self-healing function, and its durability and service life are improved.

To prepare the Fe-Al/Al$_2$O$_3$ composite coating, the powder embedding aluminizing process is mainly employed to generate a Fe-Al transition layer on the surface of metal substrate. To prevent the elevated aluminizing temperature from adversely affecting the performance of substrate material, rare earth elements are considered as additives during the aluminizing process to promote the infiltration and reduce the aluminizing temperature by their high activities[8]. The addition of rare earth elements can also increase the wear resistance[9], corrosion resistance[10], and high temperature

---

thermal stability[11] of the coating.

Subsequently, Al_2O_3 film is formed by in-situ oxidation process. Currently, the influence mechanism of rare earth elements on the growth of Al_2O_3 film has been widely researched. However, the distribution of different phases in the oxide film is rarely reported.

In this research, the phase composition of the oxide film on rare earth-modified Fe-Al/Al_2O_3 composite coating was analyzed by grazing incidence X-ray diffraction (GIXRD). Additionally, the depth distribution of elements within the oxide film was examined by Auger electron spectroscopy (AES). Furthermore, element composition and chemical structure of the oxide films at different depths were analyzed by X-ray photoelectron spectroscopy (XPS).

1 Experiment

316L stainless steel bar was processed into the disks with size of 25 mm×1 mm by wire cutting and other machining methods. Then, the disk surface was polished by 400# and 600# sandpaper to remove the deformation layer, and the ultrasonic cleaning was conducted in ethanol. Fig.1 shows the disk appearance.

Fe-Al coating was prepared through the powder pack aluminizing method. The rare earth-modified Fe-Al powder and NH_4Cl activator were used as aluminizing agents. The 316L disks and the fully mixed aluminizing powder were put into a sealed container, which was then placed in a heating furnace for embedding aluminizing process at 760 °C for 10 h. After that, the sample was cooled to room temperature and
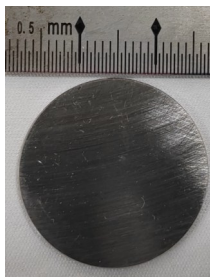

Fig.1　Appearance of disk sample

ultrasonically cleaned in ethanol. Finally, the cleaned sample was positioned in a quartz tube and heated at 760 °C for 8 h for in-situ oxidation.

The coating microstructure was analyzed by scanning electron microscope (SEM), atomic force microscope (AFM), and energy dispersive spectroscope (EDS). Meanwhile, the phase of the aluminizing layer was investigated by X-ray diffraction (XRD) analysis and GIXRD was employed to analyze the phase of oxide film. Furthermore, AES was adopted to investigate the depth distribution of elements in the oxide film. In addition, the composition and valence structure of the oxide film were analyzed by XPS.

2 Results and Discussion

2.1 Aluminizing layer

Fig.2a displays the cross-section microstructure of the rare earth-modified Fe-Al layer on 316L substrate. Clearly, the thickness of aluminizing layer is about 20 μm and three layers can be observed: external aluminized layer (I), transition layer (II), and internal diffusion layer (III). In layer I, Fe and Al are evenly distributed with atomic fraction ratio of 1:1, and the content of Cr and Ni is low. In layer II, the contents of Fe and Al decrease, whereas those of Cr and Ni increase. In layer III, Al content further reduces, whereas Fe content increases. Cr and Ni are evenly distributed. Ce is uniformly distributed with low content in all three layers.

Layer I and layer II are continuous and uniform with obvious layered structure divided by continuous white spots. EDS analysis results in Table 1 reveal that these white spots are Cr-rich components. During the heat treatment process, certain elements, such as Cr in 316L stainless steel matrix, tend to migrate towards defects. This phenomenon can be attributed to the fact that the interdiffusion rate of Fe and Al atoms is faster than that of Cr atoms, and Cr exhibits very limited solubility in Al matrix. As a result, Cr atoms at the defect sites are not completely diffused and dissolved to form Cr-rich components[12]. EDS results in Fig.2b illustrate that Al content in layer II decreases significantly, whereas Cr content increases rapidly. Consequently, a continuous white secondary phase emerges at the boundary between layer I and layer II.
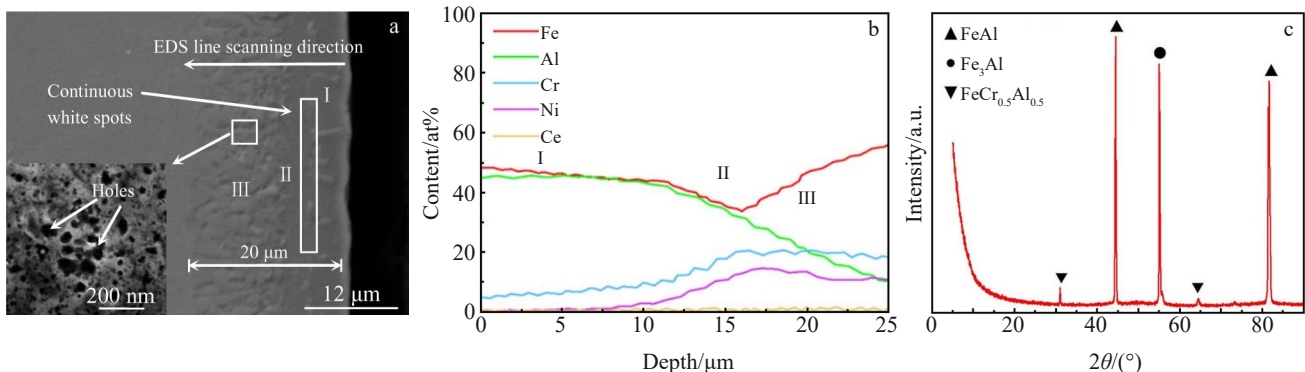

Fig.2　Cross-section microstructure (a), element distribution along depth (b), and phase composition (c) of rare earth-modified Fe-Al layer on 316L substrate

Table 1   EDS analysis results of white spots and surrounding areas in Fig.2a (at%)

Position	Fe	Al	Cr	Ni	Ce
Layer I	50.17	41.72	5.06	2.76	0.30
White spot	44.77	33.71	17.89	2.73	0.90
Layer II	44.97	38.61	5.52	10.47	0.43

Numerous holes can be observed in layer III due to the difference in atomic diffusion coefficient, the composition gradient distribution of Fe, Al, Cr, Ni, and other elements, and the accumulation of vacancies during atomic preferential diffusion[13].

According to Fig. 2c, the layer I and layer II are mainly composed of FeAl phase, whereas layer III predominantly consists of Fe_3Al phase. It can be seen that the FeAl phase mainly forms in the outer layer of the aluminizing layer. FeAl phase is an ordered intermetallic compound phase, which has good ductility and provides favorable conditions for the formation of Al_2O_3 oxide film by selective oxidation.

2.2 Oxide film

The surface morphology of Al_2O_3 film formed on the rare earth-modified Fe-Al layer is shown in Fig. 3. The oxide film exhibits a ridge structure with roughness R_a=142 nm. The transition from the unsteady phases (θ, γ) of Al_2O_3 to the steady α phase results in the volume shrinkage of approximately 13.4%, which may lead to the rough ridge structure of oxide film. Due to the fast phase transition rate, the tensile stress resulting from the instantaneous volume shrinkage becomes significant, leading to the formation of microcracks in the oxide film. Subsequently, new oxide material preferentially grows rapidly along the surfaces of
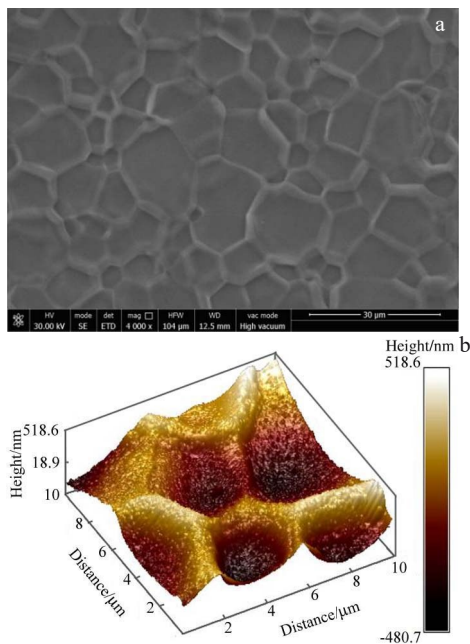
these microcracks, which extends from the crack source in oxide film to the surface of external oxide film, resulting in the formation of ridge oxide structure[14–15].

The results of element distribution along depth and phase composition of the oxide film are presented in Fig. 4. After oxidation treatment, the oxide film on the rare earth-modified Fe-Al layer has thickness of about 200 nm. The oxide film can be primarily divided into two layers: an Al-O platform layer (I) and a transition layer (II). GIXRD results indicate that the oxide film predominantly consists of α-Al_2O_3 with a small amount of γ-Al_2O_3. The FeAl phase in the aluminizing layer undergoes further diffusion, and it is transformed into the α-Fe(Al) phase during the oxidation heating process.

According to AES results, Ce content on the oxide film surface is higher but it is decreased rapidly with the increase in depth, indicating the segregation of Ce atoms. In region I (depth of 0–150 nm), Ce content is low and it is increased slightly with the increase in depth. This phenomenon suggests that Ce may contribute to the formation of a small amount of oxide in the region II. To further determine the phase composition of the surface oxide layer, the valence states of O, Fe, Al, and Ce in the oxide film were analyzed by XPS.

2.3 XPS analysis of oxide film at different depths

XPS spectra of O, Fe, Al, and Ce elements of oxide film at different depths are shown in Fig. 5 to determine the phase composition.

The binding energy of O 1s peak is 531 eV. O element exhibits the valence state of −2, and it combines with some Fe atoms, forming Fe_3O_4 at the depth of 200 nm. The binding
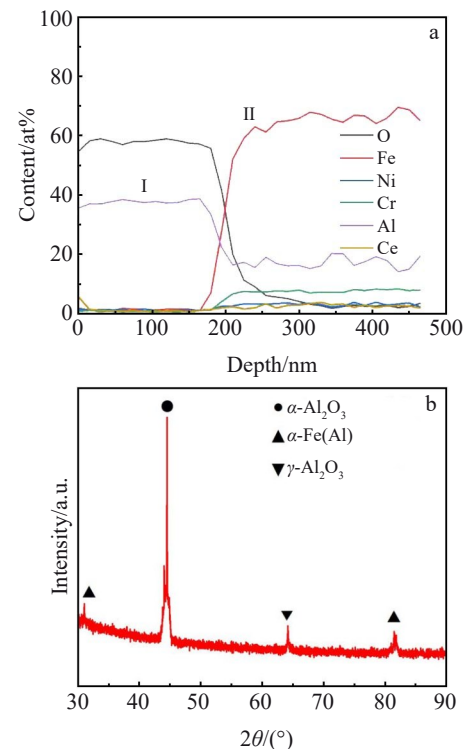

Fig.3   SEM (a) and AFM (b) surface morphologies of Al_2O_3 film formed on rare earth-modified Fe-Al layer

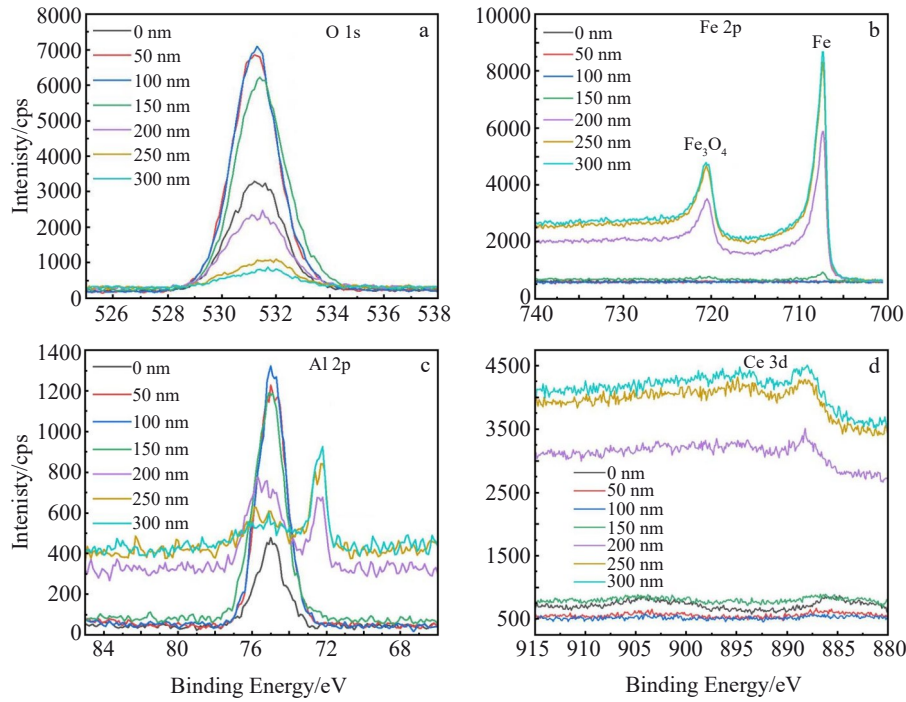Fig.4   Element distribution along depth (a) and phase composition (b) of oxide film

Fig.5   XPS spectra of rare earth-modified Al$_2$O$_3$ films: (a) O 1s, (b) Fe 2p, (c) Al 2p, and (d) Ce 3d

energy of Ce 3d and Al 2P peaks varies with depth. To accurately determine the phase composition of Ce and Al elements, the fine spectral peak fitting for Ce 3d and Al 2P was conducted in region I (depth=100 nm) and region II (depth =250 nm). The fitting results are shown in Fig.6.

It can be seen that the binding energy of Al 2p peak is 75.02 eV, corresponding to the crystal form of α-Al$_2$O$_3$. This binding

energy remains consistent with the depth further increasing to 100 nm, which is attributed to the outward diffusion of Ce from the aluminizing layer during the oxidation. Afterwards, Ce gradually accumulates on the surface, where it preferentially reacts with O$_2$ due to its higher oxygen affinity to form oxides Ce$_x$O$_y$ (Ce$_2$O$_3$, CeO$_2$)[16], as shown in Fig.7.

Pure α-Al$_2$O$_3$ is formed in the region I of the oxide film, as
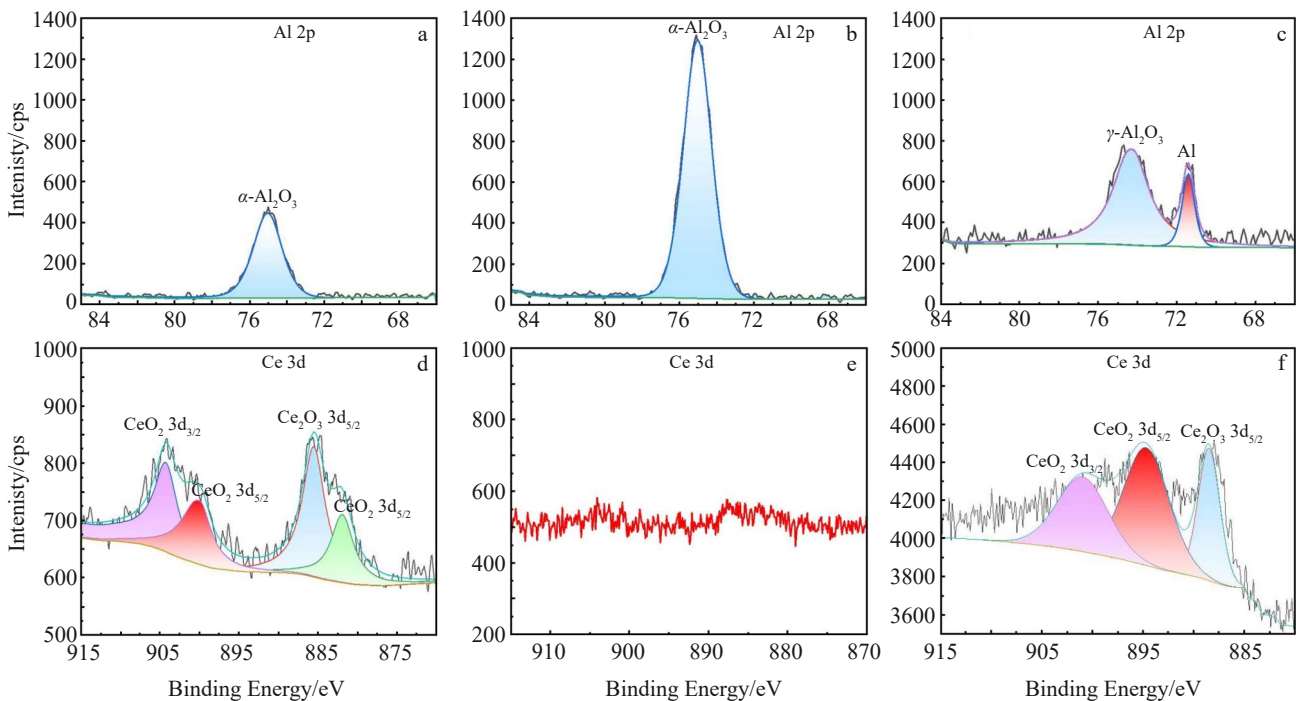

Fig.6   XPS fine spectral peak fitting results of Al element (a–c) and Ce element (d–f) on rare earth-modified Al$_2$O$_3$ films at surface (a, d), depth of 100 nm (b, e), and depth of 250 nm (c, f)
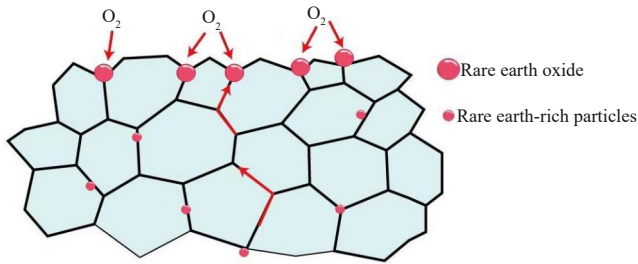
Fig.7   Schematic diagram of Ce outward diffusion and reaction with O_2

inferred in Fig. 6b and 6e. This may be because the Ce oxide has the same crystal form as α-Al_2O_3 and it is completely oxidized[17]. With the further increase in depth, dense α-Al_2O_3 appears in the oxide film and impedes the inward diffusion of O element, and the residual Al atoms appear in the region II in the oxide film. Excessive Al content hinders the formation of γ-Al_2O_3 through O combination and hinders the phase transition into α-Al_2O_3[18]. Simultaneously, Ce_xO_y exists in the transition zone where Al is not converted into α-Al_2O_3. Based on the abovementioned analysis, the thickness of oxide film is about 300 nm, and it mainly consists of α-Al_2O_3 and Ce_xO_y. At the
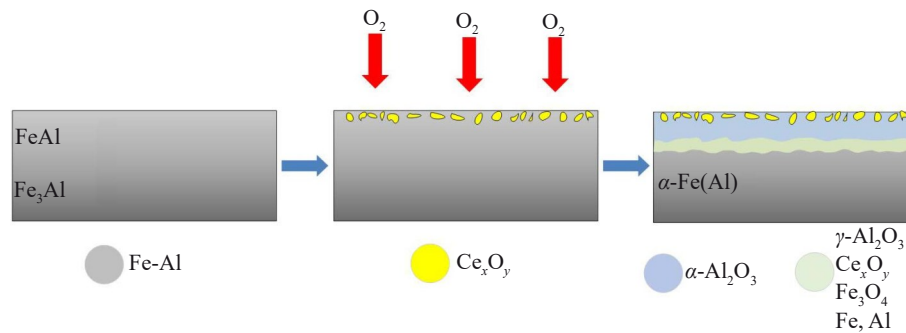

Fig.8   Schematic diagram of phase composition of oxide film

depth of about 150 nm, α-Al_2O_3 film is formed on the surface of oxide film. At the depth of 150–300 nm, the oxide film mainly consists of the transition layer, which contains mixed oxides (γ-Al_2O_3, Ce_xO_y, and Fe_3O_4), pure Fe, and pure Al, as shown in Fig.8.

3 Conclusions

1) The rare earth-modified aluminizing layer can be divided into three layers: an external aluminizing layer (I), a transition layer (II), and an internal diffusion layer (III). The continuous Cr-rich components are primarily concentrated at the interface of layer I and layer II. Numerous holes exist in the layer III.

2) The aluminizing layer is mainly composed of FeAl phase and Fe_3Al phase. The FeAl phase is predominantly formed in the outermost layer of the aluminizing layer, providing favorable conditions for the formation of Al_2O_3 oxide film by selective oxidation.

3) The surface of the oxide film presents a typical ridge structure of α-Al_2O_3. Due to the outward diffusion of Ce to the surface, Ce preferentially reacts with O_2 during the initial oxidation stage, forming Ce oxides.

4) The oxide film can be divided into two layers: a pure α-Al_2O_3 layer and a transition layer. The transition layer primarily consists of α-Fe(Al) and mixed oxides of Al, Fe, and Ce.

References

1   Causey R A, Karnesky R A, Marchi C S. *Comprehensive Nuclear Materials*[J], 2012, 4: 511

2   Devia D M, Restrepo-Parra E, Arangcr P J. *Applied Surface Science*[J], 2011, 258(3): 1164

3   Nemani V, Mcguiness P J, Daneu N *et al*. *Journal of Alloys and Compounds*[J], 2012, 539: 184

4   Zhang Junmin, Chen Xiaowu, Yang Jinshan *et al*. *Materials China*[J], 2023, 42(6): 456 (in Chinese)

5   Zhang G K, Chen C A, Luo D L *et al*. *Fusion Engineering & Design*[J], 2012, 87(7–8): 1370

6   Benamati A, Ciampichetti A, Benamati G. *Journal of Nuclear Materials*[J], 2004, 329–333(B): 1398

7   Benamati G, Chabrol C, Perujo A *et al*. *Journal of Nuclear Materials*[J], 1999, 271: 391

8   Zheng Liwei, Liu Enze, Zheng Zhi *et al*. *Rare Metal Materials and Engineering*[J], 2023, 52(12): 4117 (in Chinese)

9   Chang Weihang, Cai Haichao, Xue Yujun *et al*. *Rare Metal Materials and Engineering*[J], 2023, 52(2): 527 (in Chinese)

10   Xin Jiangping, Hui Shuiping, Zhang Siyuan *et al*. *Rare Metal Materials and Engineering*[J], 2022, 51(5): 1887 (in Chinese)

11   Wang Xin, Xue Zhaolu, Liu Xia *et al*. *Rare Metal Materials and Engineering*[J], 2022, 51(9): 3427 (in Chinese)

12   Wang Y D, Wang J X, Hu H T *et al*. *Vacuum*[J], 2018, 158: 101

13   Martin E, Helmut M. *Philosophical Magazine A*[J], 2000, 80(5): 1219

14   Peng X, Li T, Pan W P. *Scripta Materialia*[J], 2001, 44(7): 1033

15   Jiang H X, Li S X, Zhang L L. *Journal of Alloys and Compounds*[J], 2021, 859: 157804

16   Pint B A. *Oxidation of Metals*[J], 1996, 45(1): 1

17   Wang Y D, Zhang Y P, Liang G *et al*. *Vacuum*[J], 2020, 176: 109148

18   Zhou W, Zhao Y G, Li W *et al*. *Materials Science and Engineering A*[J], 2007, 458(1–2): 34

稀土改性 Fe-Al 层表面 Al$_2$O$_3$ 薄膜的物相分布

尹　琦，袁晓明，张建通，冯　凡，杨洪广

(中国原子能科学研究院，北京　102413)

摘　要：在760 ℃下采用稀土改性包埋渗铝以及原位氧化方法制备Fe-Al/Al$_2$O$_3$复合涂层，研究了渗铝层和氧化膜的微观组织和相分布。结果表明，稀土改性渗铝层可分为3层：外层渗铝层、过渡层和内扩散层。渗铝层主要由FeAl相和Fe$_3$Al相组成。FeAl相主要集中在渗铝层的外层，为Al$_2$O$_3$氧化膜的选择性氧化提供了有利条件。氧化膜表面呈α-Al$_2$O$_3$脊状结构。此外，表面氧化铈的存在是由于氧化初期Ce向外扩散且与O$_2$的优先反应。氧化膜可分为2层，即纯α-Al$_2$O$_3$层和主要由α-Fe(Al)和Al、Fe、Ce的混合氧化物组成的过渡层。

关键词：稀土改性；渗铝层；氧化膜；物相分布

作者简介：尹　琦，男，1999年生，硕士，中国原子能科学研究院，北京　102413，E-mail：13124781761@163.com